

---

# MHD Flow of Second Grade Fluid with Heat Absorption and Chemical Reaction

Muhammad Ramzan<sup>1,\*</sup>, Ahmad Shafique<sup>1</sup>, Mudassar Nazar<sup>1,2</sup>

<sup>1</sup>Centre for Advanced Studies in Pure and Applied Mathematics, Bahauddin Zakariya University, Multan, Pakistan

<sup>2</sup>School of Mathematical Sciences, University of Science and Technology of China, Hefei, China

## Email address:

muhammadramzan4434445@gmail.com (M. Ramzan), ahmadshafique1032@gmail.com (A. Shafique),

mudassar\_666@yahoo.com (M. Nazar)

\*Corresponding author

## To cite this article:

Muhammad Ramzan, Ahmad Shafique, Mudassar Nazar. MHD Flow of Second Grade Fluid with Heat Absorption and Chemical Reaction. *International Journal of Theoretical and Applied Mathematics*. Vol. 8, No. 2, 2022, pp. 30-39. doi: 10.11648/j.ijtam.20220802.11

**Received:** January 26, 2022; **Accepted:** March 2, 2022; **Published:** March 18, 2022

---

**Abstract:** The objective of this paper is to analyze the influence of thermo-diffusion on magnetohydrodynamics (MHD) flow of fractional second grade fluid immersed in a porous media over an exponentially accelerated vertical plate. In addition, other factors such as heat absorption and chemical reaction are used in the problem. More exactly, the fractional model has been developed using the generalized Fick's and Fourier's laws. The Caputo-Fabrizio (CF) fractional derivative has been used to solved the model. Initially, the flow modeled system of partial differential equations are transformed into dimensional form through suitable dimensionless variable and then Laplace transform technique has been used to solved the set of dimensionless governing equations for velocity profile, temperature profile, and concentration profile. The influence of different parameters like diffusion-thermo, fractional parameter, magnetic field, chemical reaction, heat absorption, Schmidt number, time, Prandtl number and second grade parameter are discussed through numerous graphs. From figures, it is observed that fluid motion decreases with increasing values of Schmidt number, Prandtl number, magnetic parameter, and chemical reaction, whereas velocity field decreases with decreasing values of diffusion-thermo and mass grashof number. In order to check the authenticity of present work, we compare the present work with already published model graphically.

**Keywords:** Free Convection, Chemical Reaction, Diffusion-thermo, Magnetic Field

---

## 1. Introduction

Now a days, magnetohydrodynamic (MHD) has been extended into wide areas of basic and applied research in sciences and engineering. The study of non-Newtonian fluid becomes very interested due to variety of technological applications like making of plastic sheets, lubricant's performance and motion of biological fluid.

Numerous fluid models have been presented to demonstrate the distinction between Newtonian and non-Newtonian fluids. Kai-Long Hsiao [1] worked on magnetohydrodynamics Maxwell fluid. Shah et al. [2] discussed the influence of magnetic field of fractional order. The model on Jeffrey fluid be the simplest and most popular, and it has attracted the interest of researchers in the field. Some of the work on Jeffrey fluid are of Das [3] and Qasim [4]. Ahmad et al. [5] compared the

generalized form of Jeffrey fluid flow acquired by contemplating fractional derivative of singular kernel (Caputo) and non-singular kernel (Caputo-Fabrizio). During the last decade, different generalized fractional derivatives have appeared in the literature that are derivatives of Caputo, Caputo-Fabrizio, constant proportional Caputo [6, 7]. Some studies of free convection on an inclined plane invarious thermal and mechanical situations have recently been presented by mathematicians [8-14]. Some mathematical models of second grade fluids are industrial oils, slurry streams, and dilute polymer solutions with different geometry and boundary conditions. The Sheikh et al. [15] discussed the casson fluid. Ahmed et al. [16] has analyzed MHD heat transfer into convective boundary layer with a minimal pressure gradient. Convective mixed MHD flow studied by Narayana [17], while Authors in [18] worked on MHD fluid over a plate. Khan et al. [19] presented a fractional flow of fluid on a vertical surface

driven by temperature as well as concentration gradients. Khan *et al.* [20] discussed magnetohydrodynamic flow in the existence of permeable media through plate. Seth *et al.* [21] discussed the magnetohydrodynamics flow over a plate. Tran *et al.* [22] worked on mandatory stability of fractional derivatives for fractional calculus equations, and the mathematical model used for transference of COVID-19 with Caputo fractional derivatives also discussed by Tuan *et al.* [23].

Y. Liu *et al.* [24] presented the flow of fluid using a heat generation. Ramzan *et al.* [25] reported the behaviour of heat consumption/generation on the MHD flow of Brinkman fluid. Khan *et al.* [26] investigated the Brinkman fluid effect between two side walls. Ali *et al.* [27] discussed on the magnetohydrodynamics fluid with heat transport. Ahmad *et al.* [28] discussed the nanofluid over a plate. Sheikh *et al.* [29] studied the MHD flow with heat transfer. Ahmat *et al.* [30] discussed the flow over a heated plate. Ali *et al.* [31] studied the water based fluid. Razzaq *et al.* [32] discussed the nanofluid with newtonian heating over a plate.

In this problem, an unsteady MHD flow of second grade fluid over a vertical plate is considered with Dufour effect.

$$\frac{\partial u_1(x^*, t_1^*)}{\partial t_1^*} = (1 + \beta_0 \frac{\partial}{\partial t_1^*}) \frac{\partial \tau(x^*, t_1^*)}{\partial x^*} + g\beta_{T^*}(T^* - T_\infty^*) - \frac{\sigma\beta_0^2 u_1(x^*, t_1^*)}{\rho} - \frac{\mu u_1(x^*, t_1^*)}{\rho K_2} + g\beta_{C^*}(C^* - C_\infty^*) \tag{1}$$

shear stress  $\tau$  is:

$$\tau = \nu \frac{\partial u_1(x^*, t_1^*)}{\partial x^*} \tag{2}$$

Thermal Eq. is:

$$\frac{\partial T^*(x^*, t_1^*)}{\partial t_1^*} = -\frac{1}{\rho c_p} \frac{\partial q_1(x^*, t_1^*)}{\partial x^*} - Q_1(T^* - T_\infty^*) - \frac{D_0 K_T \rho}{c_s} \frac{\partial J_1(x^*, t_1^*)}{\partial x^*} \tag{3}$$

According to Fourier's Law:

$$q_1(x^*, t_1^*) = -\alpha_0 \frac{\partial T^*(x^*, t_1^*)}{\partial x^*} \tag{4}$$

Diffusion Eq. is:

$$\frac{\partial C^*(x^*, t_1^*)}{\partial t_1^*} = -\frac{\partial J_1(x^*, t_1^*)}{\partial x^*} - R_1(C^* - C_\infty^*) \tag{5}$$

$J_1(x^*, t_1^*)$  defined by Fick, s law:

$$J_1(x^*, t_1^*) = -D_m \frac{\partial C^*(x^*, t_1^*)}{\partial x^*} \tag{6}$$

The conditions for model are:

$$u_1(x^*, 0) = 0, T^*(x^*, 0) = T_\infty^*, C^*(x^*, 0) = C_\infty^*, x^* > 0 \tag{7}$$

$$u_1(x^*, t_1) = U_1 f(t_1^*),$$

$$T^*(x^*, t_1^*) = \begin{cases} T_\infty^* + \frac{(T_w^* - T_\infty^*)t_1^*}{t_0}, & 0 < t_1^* \leq t_0; \\ T_w^*, & t_1^* > t_0, \end{cases}$$

$$C^*(x^*, t_1^*) = C_w^*, x^* = 0 \tag{8}$$

$$u_1(x^*, t_1^*) \rightarrow 0, T^*(x^*, t_1^*) \rightarrow 0, C^*(x^*, t_1^*) \rightarrow 0,$$

$$x^* \rightarrow \infty, t_1^* > 0 \tag{9}$$

Initially, non-dimensional the giving equations and solved these equations via Laplace transform. All concentration, Temperature, and velocity distribution results have been obtained and evaluated graphically. From figures, it is seen that fluid motion decreases with larger values of Schmidt number and chemical reaction, whereas velocity field decreases with decreasing values of diffusion-thermo.

## 2. Mathematical Model

A magnetohydrodynamic flow of second grade fluid over a plate is considered. The  $y^*$ -axis is taken vertically upward along fluid motion and the  $x^*$ -axis is perpendicular to the plate. The fluid and plate have  $T_\infty^*$  concentration and  $T_\infty^*$  temperature at time  $0 = t_1^*$  with zero velocity. But for  $t_1^* > 0$ , the plate starts to move in the plane with uniform velocity  $U_1 e^{at_1^*}$ . The level of concentration is raised to  $C_w^*$  and temperature of the plate is increased or decreased to  $T_\infty^* + (T_w^* + T_\infty^*)t_1^*/t_0^*$  when  $t_1^* \leq t_0^*$  and  $T_w^*$  for  $t_1^* > t_0^*$ . In view of above assumption and using Boussinesq's approximation, linear momentum Eq. (15) is:

## 3. Generalized Model

Dimensionless parameters are:

$$x^* = \frac{Ux^*}{\nu}, t^* = \frac{U^2 t_1^*}{\nu}, u^* = \frac{u_1^*}{U}, R^* = \frac{R_1 \nu}{U^2},$$

$$Gr^* = \frac{\nu \beta_{T^*} (T_w^* - T_\infty^*)}{U^3}, Q^* = \frac{Q_0 \nu}{U^2}, C^* = \frac{C^* - C_\infty^*}{C_w^* - C_\infty^*},$$

$$M^* = \frac{\beta_0^2 \sigma}{\rho U^2}, Gm^* = \frac{\nu \beta_{C^*} (C_w^* - C_\infty^*)}{U^3} \tag{10}$$

Eq. (2) is fractionally generalized by [29, 33]

$$\tau = L_\beta D_t^\beta \frac{\partial u}{\partial x}, 1 \geq \beta > 0 \tag{11}$$

where  $L_\beta = 1$  when  $\beta \rightarrow 1$ . Put Eq. (11) into Eq. (1) and using non-dimensional parameter from Eq. (10), we found:

$$\frac{\partial u}{\partial t} = L_\beta (1 + \lambda \frac{\partial}{\partial t}) \frac{\partial}{\partial x} [D_t^\beta \frac{\partial u}{\partial x}] - (M + K^{-1})u + GrT + GmC \tag{12}$$

Eq. (4) is generalized by [34, 35]

$$q_1 = -D_\gamma D_t^\gamma \frac{\partial T}{\partial x}, 1 \geq \gamma > 0 \tag{13}$$

where thermal conductivity has generalized coefficient  $D_\gamma$ .

Eq. (6) is generalized as:

$$J_1 = -K_\alpha D_t^\alpha \frac{\partial C}{\partial x}, 1 \geq \alpha > 0 \tag{14}$$

where molecular diffusion has generalized coefficient  $K_\alpha$ . Put Eq. (14) and Eq. (15) into Eq. (3) and making non-dimensional results, we have:

$$\frac{\partial T}{\partial t} = Pr^{-1} \frac{\partial}{\partial x} [D_t^\gamma \frac{\partial T}{\partial x}] - QT + Du \frac{\partial}{\partial x} [D_t^\alpha \frac{\partial C}{\partial x}] \quad (15)$$

where  $Pr = \frac{\nu \rho C_p}{D_\gamma}$  is the generalized parameter.

Put Eq. (15) into Eq. (5) and making non-dimensional results, we have:

$$\frac{\partial C}{\partial t} = Sc^{-1} \frac{\partial}{\partial x} [D_t^\alpha \frac{\partial C}{\partial x}] - RC \quad (16)$$

where  $Sc = \frac{\nu}{K\alpha}$  is the generalized parameter.

with the following conditions:

$$u(x, t) = T(x, t) = C(x, t) = 0, x > 0, t = 0 \quad (17)$$

$$u(0, t) = e^{at},$$

$$T(0, t) = \begin{cases} t, & 0 < t \leq 1; \\ 1, & t > 1, \end{cases} C(0, t) = 1, t > 0 \quad (18)$$

$$u(x, t) \rightarrow 0, T(x, t) \rightarrow 0, C(x, t) \rightarrow 0, x \rightarrow \infty \quad (19)$$

where  $Gm, \lambda, M, Q, Du,$  and  $u$  represents the mass Grashof number, second grade parameter, magnetic field, non-dimensional heat absorption parameter, Diffusion-thermo parameter, and motion of fluid respectively. and  $D_t^\beta f(t)$  reports the (CF) derivative of  $f(t)$  as:

$$D_t^\beta f(t) = \frac{1}{(1-\beta)} \int_0^t (e^{-\frac{\beta(r-t)}{1-\beta}}) f'(r) dt \quad (20)$$

$$\bar{T}(x, s) = \frac{1-e^{-s}}{s^2} e^{-x\sqrt{\frac{Pr}{s}(s+Q)(\gamma+s(1-\gamma))}} + \frac{PrScDu(s+R)}{s^2(\gamma+s(1-\gamma))} [e^{-x\sqrt{\frac{Pr}{s}(s+Q)(\gamma+s(1-\gamma))}} - e^{-x\sqrt{\frac{Sc}{s}(s+R)(\alpha+s(1-\alpha))}}] \quad (26)$$

for  $\alpha = \gamma$ , suitable form of Eq. (26) is:

$$\bar{T}(x, s) = \frac{1-e^{-s}}{s^2} e^{-x\sqrt{\frac{Pr}{s}(s+Q)(\alpha+s(1-\alpha))}} + \frac{PrScDu(s+R)}{s^2(\alpha+s(1-\alpha))} [e^{-x\sqrt{\frac{Pr}{s}(s+Q)(\alpha+s(1-\alpha))}} - e^{-x\sqrt{\frac{Sc}{s}(s+R)(\alpha+s(1-\alpha))}}] \quad (27)$$

The semi-analytical solution of Eq. (27) is given by algorithm [37, 38].

### 4.3. Calculation of Velocity

Applying Laplace transform on Eq. (12), we have:

$$s\bar{u}(x, s) = L_\beta(1 + \lambda s) \left( \frac{s}{\beta+s(1-\beta)} \right) \frac{\partial^2 \bar{u}(x, s)}{\partial x^2} - (M + K^{-1})\bar{u}(x, s) + Gr\bar{T}(x, s) + Gm\bar{C}(x, s) \quad (28)$$

with conditions

$$\bar{u}(0, s) = \frac{1}{s-a}, \bar{u}(x, s) \rightarrow 0, x \rightarrow \infty \quad (29)$$

Put Eq. (29) in Eq. (28), we obtain:

$$\bar{u}(x, s) = \frac{1}{s-a} e^{-x\sqrt{\frac{(M+s+\frac{1}{K})(\beta+s(1-\beta))}{s(1+\lambda s)L_\beta}}} + \left[ \frac{Gr}{L_\beta \left[ \frac{s(1+\lambda s)}{\beta+s(1-\beta)} \right] \left[ \frac{\alpha+(1-\alpha)}{s} \right] (R+s)Pr-(s+M+K^{-1})} \right] \left[ \frac{1-e^{-s}}{s^2} + \frac{PrScDu(R+s)}{s^2(\alpha+s(1-\alpha))} \right] \left[ e^{-x\sqrt{\frac{(M+s+\frac{1}{K})(\beta+s(1-\beta))}{s(1+\lambda s)L_\beta}}} - e^{-x\sqrt{\frac{Pr}{s}(Q+s)(\alpha+s(1-\alpha))}} \right] + \left[ \frac{1}{L_\beta \left[ \frac{s(1+\lambda s)}{\beta+s(1-\beta)} \right] \left[ \frac{\alpha+(1-\alpha)}{s} \right] (R+s)Sc-(M+s+K^{-1})} \right] \left[ \frac{Gm}{s} - \frac{GrPrScDu(R+s)}{s^2(\alpha+s(1-\alpha))} \right] \left[ e^{-x\sqrt{\frac{(s+\frac{1}{K}+M)(\beta+s(1-\beta))}{s(1+\lambda s)L_\beta}}} - e^{-x\sqrt{\frac{Sc}{s}(R+s)(\alpha+s(1-\alpha))}} \right] \quad (30)$$

## 4. Solution of Problem

### 4.1. Calculation of Concentration

Applying Laplace transform on Eq. (16), we have:

$$s\bar{C}(x, s) = Sc^{-1} \left( \frac{s}{\alpha+s(1-\alpha)} \right) \frac{\partial^2 \bar{C}(x, s)}{\partial x^2} - \bar{C}(x, s)R \quad (21)$$

with

$$\bar{C}(0, s) = s^{-1}, \bar{C}(x, s) \rightarrow 0, x \rightarrow \infty \quad (22)$$

Put Eq. (22) in Eq. (21), we have:

$$\bar{C}(y, s) = s^{-1} e^{-x\sqrt{(s+R)Sc\left(\frac{\alpha+s(1-\alpha)}{s}\right)}} \quad (23)$$

The semi-analytical solution of Eq. (23) is given by algorithm [37, 38].

### 4.2. Calculation of Temperature

Applying Laplace transform on Eq. (15), we have:

$$s\bar{T} = Pr^{-1} \left( \frac{s}{\gamma+s(1-\gamma)} \right) \frac{\partial^2 \bar{T}}{\partial x^2} - Q\bar{T} + Du \left( \frac{s}{\alpha+s(1-\alpha)} \right) \frac{\partial^2 \bar{C}}{\partial x^2} \quad (24)$$

with

$$\bar{T}(0, s) = s^{-2}(1 - e^{-s}), \bar{T}(x, s) \rightarrow 0, x \rightarrow \infty \quad (25)$$

Put Eq. (25) in Eq. (24), which result is:

for  $\alpha = \beta = \gamma$ , suitable form of Eq. (30) is:

$$\begin{aligned} \bar{u}(x, s) = & \frac{1}{s-a} e^{-x \sqrt{\frac{(s+M+\frac{1}{K})(\alpha+s(1-\alpha))}{s(1+\lambda s)L_\beta}}} + \left[ \frac{Gr}{(1+\lambda s)L_\beta(s+Q)Pr-(s+M+K^{-1})} \right] \left[ \frac{1-e^{-s}}{s^2} + \frac{PrScDu(s+R)(\alpha+s(1-\alpha))}{Sc(R+s)-Pr(Q+s)} \right] e^{-x \sqrt{\frac{(s+M+\frac{1}{K})(\alpha+s(1-\alpha))}{s(1+\lambda s)L_\beta}}} - \\ & e^{-x \sqrt{\frac{Pr(s+Q)(\alpha+s(1-\alpha))}{s}}} + \left[ \frac{1}{(1+\lambda s)L_\beta(s+R)Sc-(s+M+K^{-1})(1+\lambda s)} \right] \left[ \frac{Gm}{s} - \frac{GrPrScDu(s+R)(\alpha+s(1-\alpha))}{Sc(s+R)-Pr(s+Q)} \right] e^{-x \sqrt{\frac{(s+M+\frac{1}{K})(\alpha+s(1-\alpha))}{s(1+\lambda s)L_\beta}}} - \\ & e^{-x \sqrt{\frac{Sc(s+R)(\alpha+s(1-\alpha))}{s}}} \end{aligned} \tag{31}$$

The semi -analytical solution of Eq. (31) is given by algorithm [37, 38].

### 5. Results and Discussion

The solution for the impact of diffusion-thermo, magnetic field, and heat consumption on flow of second grade fluid past over a vertical plate are developed by using Laplace transform technique. The effect of numerous parameters used in the governing equations of velocity fields have been analyzed in Figures.

The impact of  $M$  on  $u(x, t)$  is reported in Figure 1. Graph shows that fluid speed  $u(x,t)$  is reduced with accelerating values of parameter  $M$ . Resistivity becomes dominant with raising  $M$  which reduced the speed of fluid. Figure 2 indicates the effect of porosity on velocity fields. It is noted from this Figure that speed of fluid becomes higher for larger values of  $K$ . Physically, it happened that the resistivity of porous medium is higher for lower values of  $K$  which decreased the flow regime.

Figure 3 represent the result of  $Gr$  on fluid velocity  $u(x,t)$ . The fluid motion rises up with maximizing the values of  $Gr$ , and it represents the impact of thermal buoyancy force to viscous force. Therefore maximizing the values of  $Gr$  exceed the temperature gradient due to which velocity field rises. The impact of  $Gm$  on fluid velocity  $u(x, t)$  is illustrate in Figure 4. It is highlighted that fluid motion raises as values of  $Gm$  increasing. Physically higher the values of  $Gm$  increase the concentration gradients which make the buoyancy force significant and hence it is examined that velocity field is raising.

The effects of  $Du$  on  $u(x,t)$  is shown in Figure 5. Figure shows that speed of fluid increases by increasing value of  $Du$ . The reason behind this is that the rate of mass diffusion is raised with an increasing value of  $Du$ , which decreases the fluid viscosity and hence velocity of fluid is increased. Figure 6 is drawn for negative values of  $Du$  which shows the opposite behavior.

A decreasing value of  $Q$  increases the  $u(x,t)$  as appeared in Figure 7. An increasing value of  $R$  decreases the  $u(x,t)$  as appeared in Figure 8.

Figure 9 represents the behavior of  $Sc$  on the  $u(x, t)$ . It is highlighted that maximizing the values of  $Sc$  slow down the fluid motion due to decay of molecular diffusion. The impact of  $Pr$  on  $u(x,t)$  is displayed in Figure 10. Figure 11 highlight the behavior of  $t$  on  $u(x,t)$ . From Figure, it is observed that  $u(x, t)$  is accelerated for larger time  $t$ . Figure 12 shows the influence of  $\alpha$  on  $u(x, t)$ . From Figure, it is

noted that fluid motion  $u(x, t)$  decays with raising values of  $\alpha$ .

The behavior of parameter  $Pr$  on  $T(x, t)$  is reported in Figure 13. This Figure indicates that temperature decreases with larger  $Pr$ . Figure 14 indicates the impact of  $Q$  on  $T(x, t)$ . Figure 15 indicates the effect of  $Sc$  on  $T(x, t)$ . Temperature increases with reducing values of  $Sc$  as highlight in Figure 16 indicates the impact of  $Du$  on  $T(x, t)$ . Temperature rises with increasing  $Du$ . Figure 17 shows the effect of  $t$  on  $T(x, t)$ . From Figure, it is noted that  $T(x, t)$  falls down with reducing values of time  $t$ . Figure 18 shows the influence of  $\alpha$  on  $T(x, t)$ . From Figure, it is noted that  $T(x, t)$  decays down for larger values of  $\alpha$ .

Figure 19 shows the influence of  $\alpha$  on  $C(x, t)$ . From Figure, it is noted that concentration level decays down with raising values of  $\alpha$ . Figure 20 shows the influence of  $t$  on  $C(x, t)$ . From Figure, it is noted that concentration level rises with raising time  $t$ . The behavior of  $R$  on  $C(x, t)$  are shown in Figure 21. Figure 22 shows the effect of  $Sc$  on  $C(x, t)$ . Figures 23 to 25 represents the authenticity of inversion algorithms for  $C(x,t)$ ,  $T(x,t)$ , and  $u(x,t)$ . Figure 26 gives the comparison of present work with Shah *et al.* [36]. Figure represents that in the absence of fractional parameters, dufour effect, second grade parameter, and porous media, we obtained the identical fluid motion.

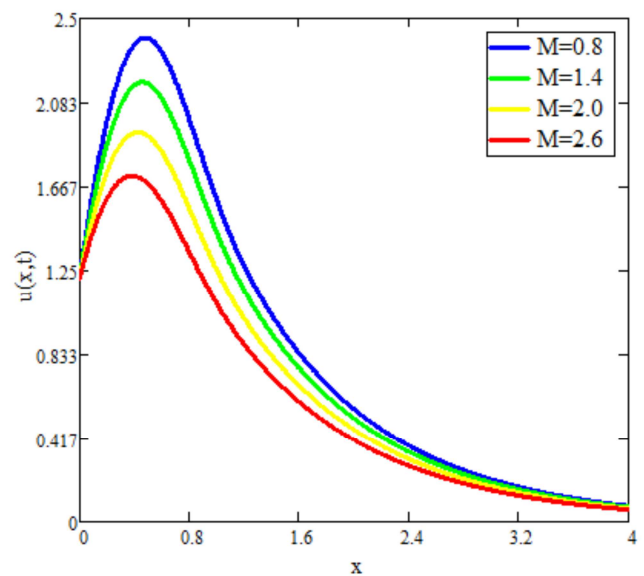
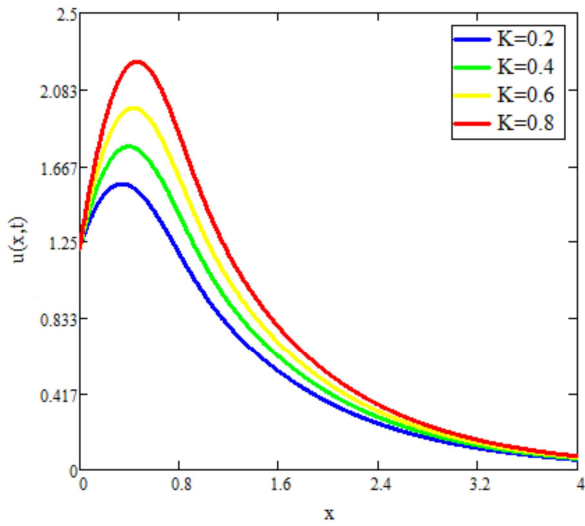
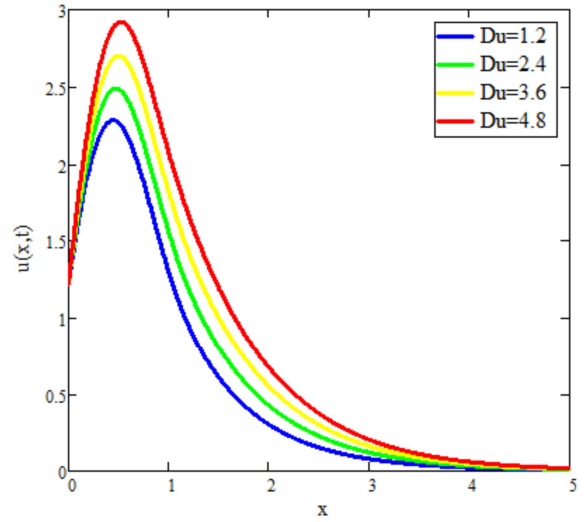


Figure 1. Velocity profile  $u(x,t)$  for parameter  $M$  at  $R=1.2, Q=4, Gr=6, Gm=6, Du=2, Sc=2.5, Pr=0.5, K=3$ .



**Figure 2.** Velocity profile  $u(x,t)$  for parameter  $K$  at  $R=1.2, Q=4, Gr=6, Gm=6, Du=2, Sc=2.5, Pr=0.5, M=0.4$ .



**Figure 5.** Velocity profile  $u(x,t)$  for parameter  $Du$  at  $R=1.2, Q=4, Gr=6, Gm=6, K=3, Sc=2.5, Pr=0.5, M=0.4$ .

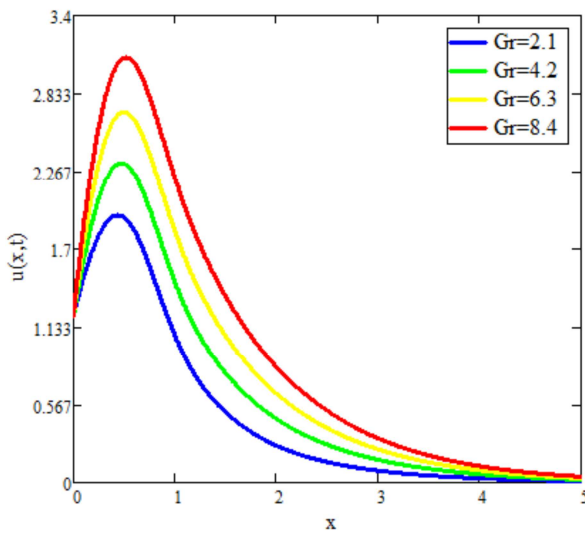


**Figure 3.** Velocity profile  $u(x,t)$  for parameter  $Gr$  at  $R=1.2, Q=4, K=3, Gm=6, Du=2, Sc=2.5, Pr=0.5, M=0.4$ .

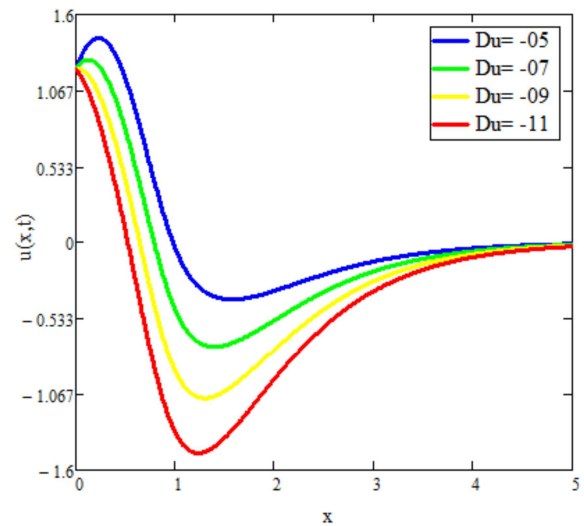


**Figure 6.** Velocity profile  $u(x,t)$  for parameter  $Du$  at  $R=1.2, Q=4, Gr=6, Gm=6, K=3, Sc=2.5, Pr=0.5, M=0.4$ .

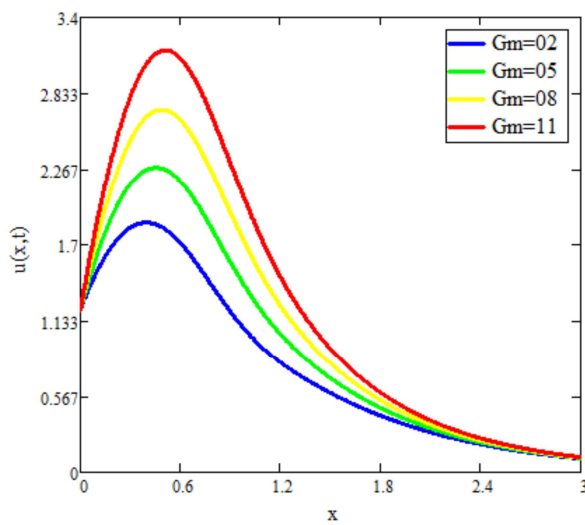


**Figure 4.** Velocity profile  $u(x,t)$  for parameter  $Gm$  at  $R=1.2, Q=4, Gr=6, K=3, Du=2, Sc=2.5, Pr=0.5, M=0.4$ .

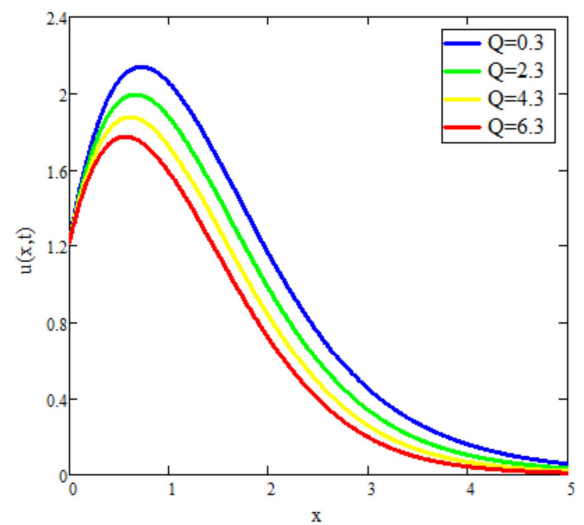


**Figure 7.** Velocity profile  $u(x,t)$  for parameter  $Q$  at  $R=1.2, Du=2, Gr=6, Gm=6, K=3, Sc=2.5, Pr=0.5, M=0.4$ .

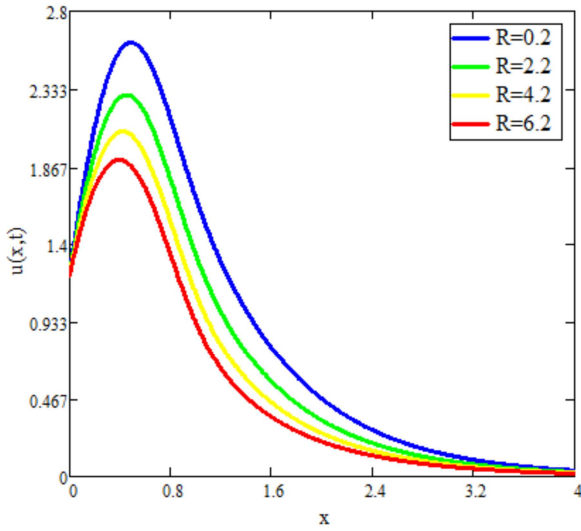


**Figure 8.** Velocity profile  $u(x,t)$  for parameter  $R$  at  $Gm=1.2, Q=4, Gr=6, K=3, Du=2, Sc=2.5, Pr=0.5, M=0.4$ .

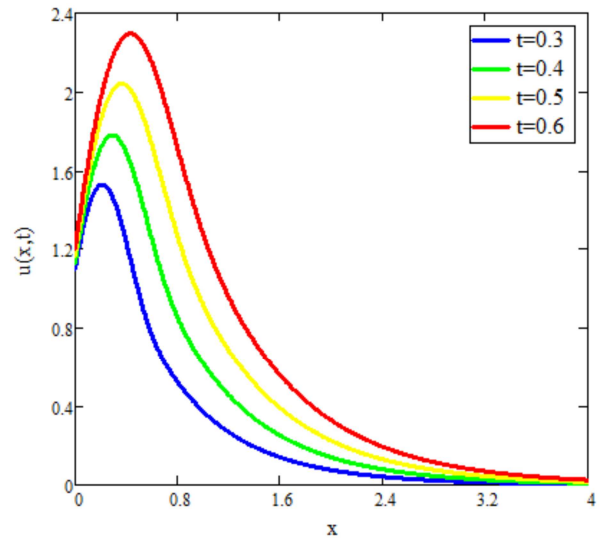


**Figure 11.** Velocity profile  $u(x,t)$  for parameter  $t$  at  $R=1.2, Q=4, Gr=6, K=3, Du=2, Sc=2.5, Pr=0.5, M=0.4$ .

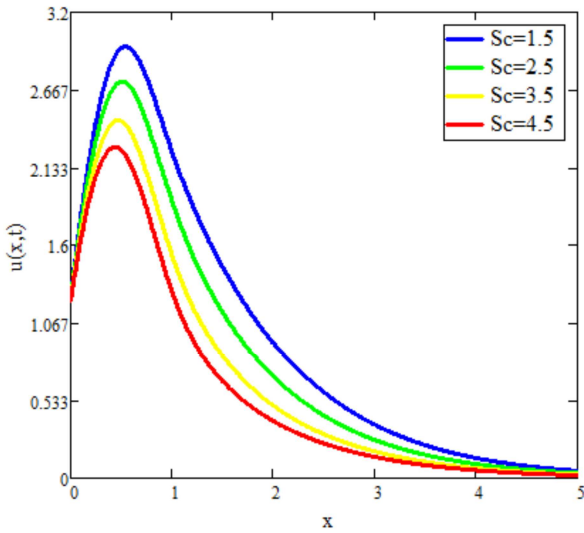


**Figure 9.** Velocity profile  $u(x,t)$  for parameter  $Sc$  at  $R=1.2, Q=4, Gr=6, K=3, Du=2, Gm=6, M=0.4, Pr=0.5$ .

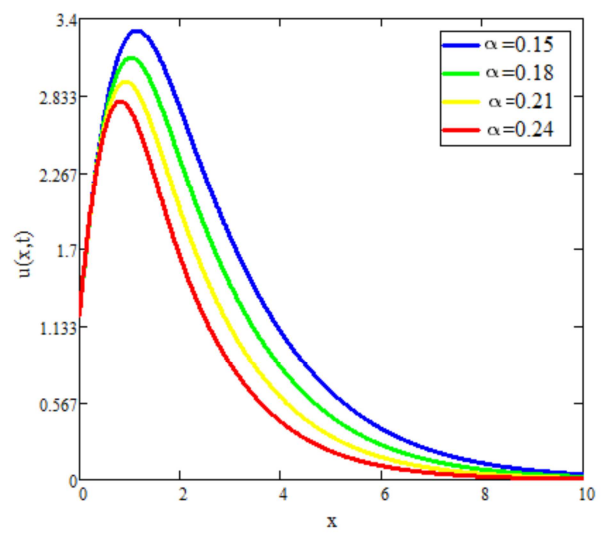


**Figure 12.** Velocity profile  $u(x,t)$  for parameter  $\alpha$  at  $R=1.2, Q=4, Gr=6, K=3, Du=2, Sc=2.5, Pr=0.5$ .

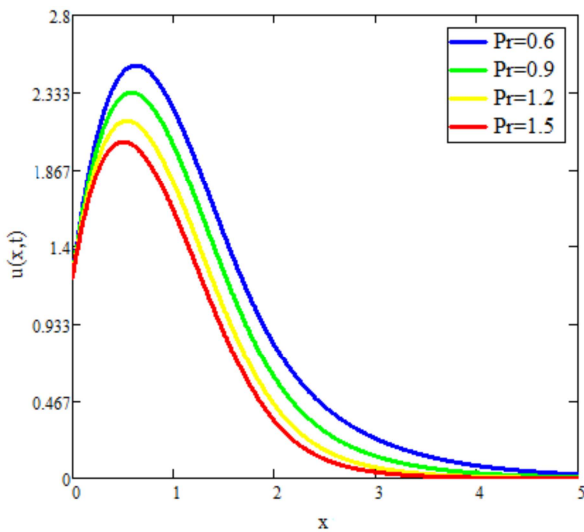


**Figure 10.** Velocity profile  $u(x,t)$  for parameter  $Pr$  at  $R=1.2, Q=4, Gr=6, K=3, Du=2, Sc=2.5, Gm=6, M=0.4$ .

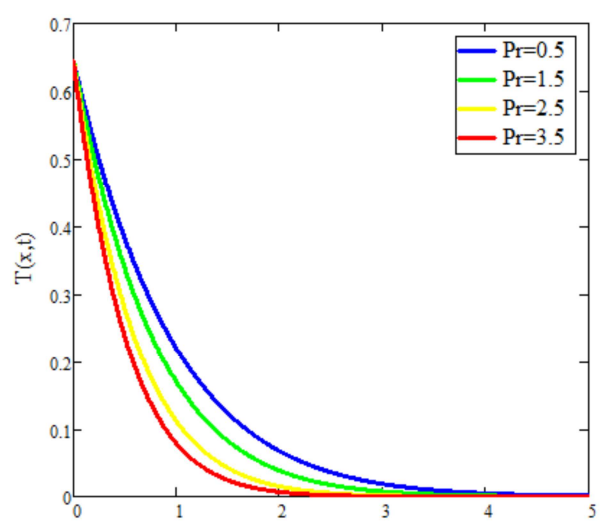


**Figure 13.** Temperature profile  $T(x,t)$  for parameter  $Pr$  at  $R=1.2, Q=4, t=0.65, Sc=2.5, \beta=0.5$ .

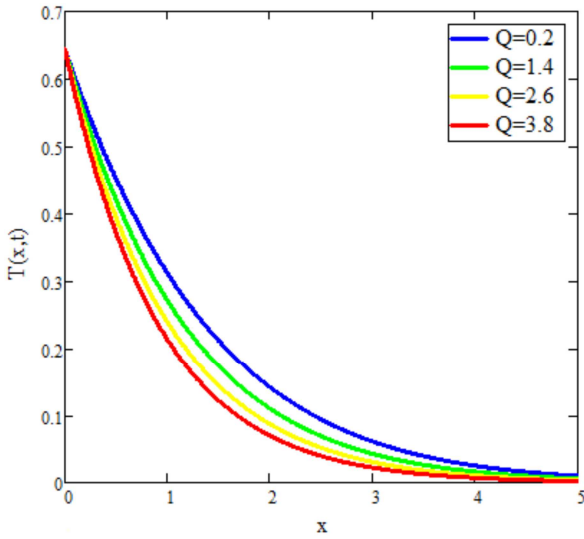


Figure 14. Temperature profile  $T(x,t)$  for parameter  $Q$  at  $R=1.2$ ,  $Pr=0.5$ ,  $t=0.65$ ,  $Sc=2.5$ ,  $\beta=0.5$ ,  $Du=2$ .

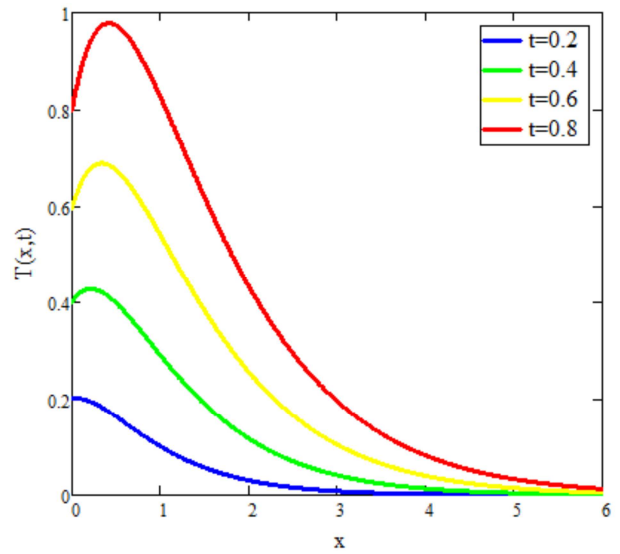


Figure 17. Temperature profile  $T(x,t)$  for parameter  $t$  at  $R=1.2$ ,  $Q=4.0$ ,  $t=0.65$ ,  $Sc=2.5$ ,  $\beta=0.5$ .

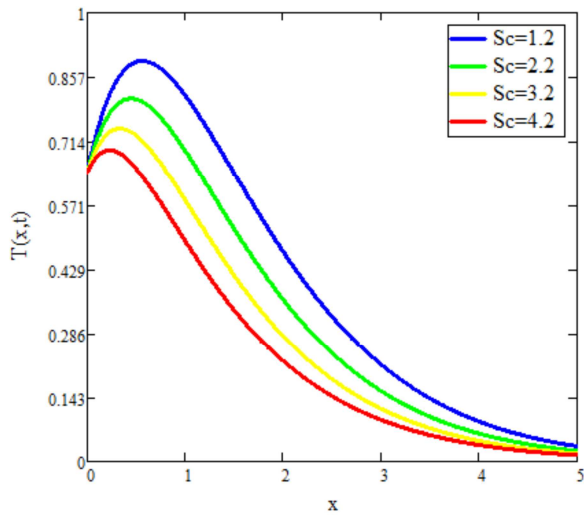


Figure 15. Temperature profile  $T(x,t)$  for parameter  $Sc$  at  $R=1.2$ ,  $Q=4$ ,  $t=0.65$ ,  $Du=2$ ,  $\beta=0.5$ ,  $Pr=0.5$ .

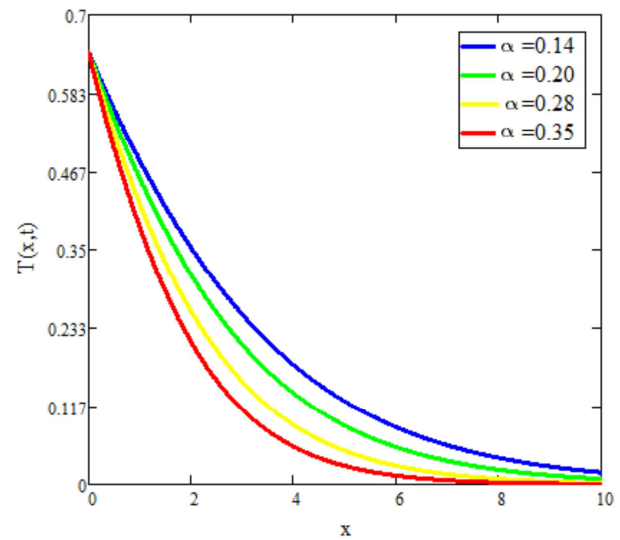


Figure 18. Temperature profile  $T(x,t)$  for parameter  $\alpha$ .

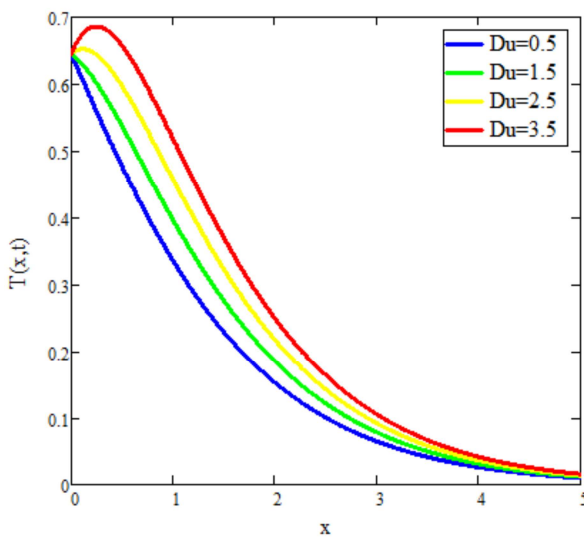


Figure 16. Temperature profile  $T(x,t)$  for parameter  $Du$  at  $R=1.2$ ,  $Q=4$ ,  $t=0.65$ ,  $Sc=2.5$ ,  $\beta=0.5$ ,  $Pr=0.5$ .

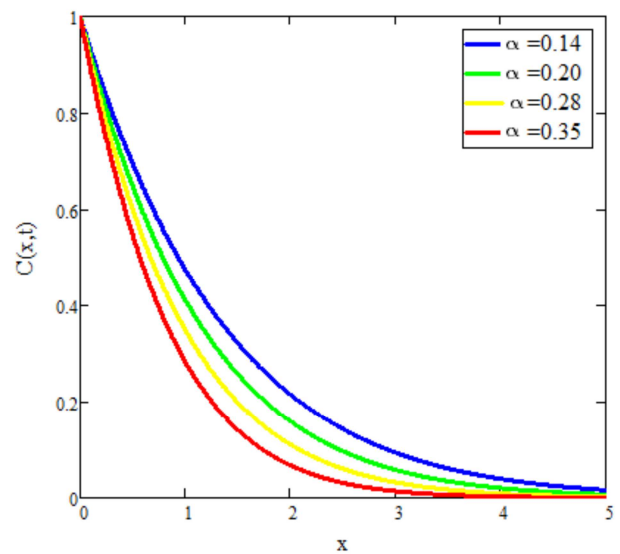


Figure 19. Concentration profile  $C(x,t)$  for parameter  $\alpha$ .

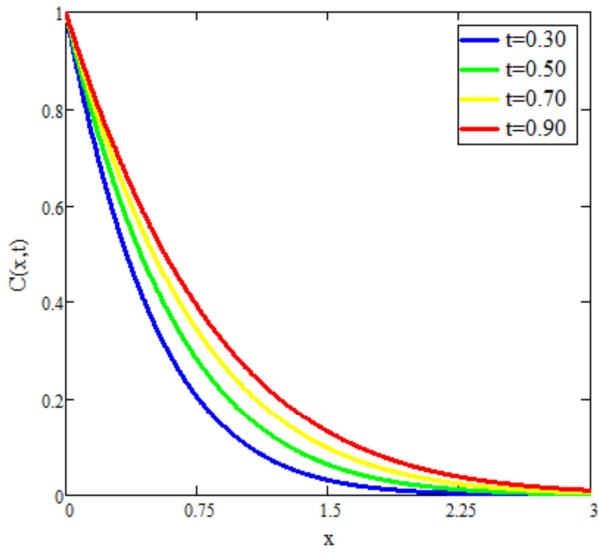


Figure 20. Concentration profile  $C(x,t)$  for parameter  $t$ .

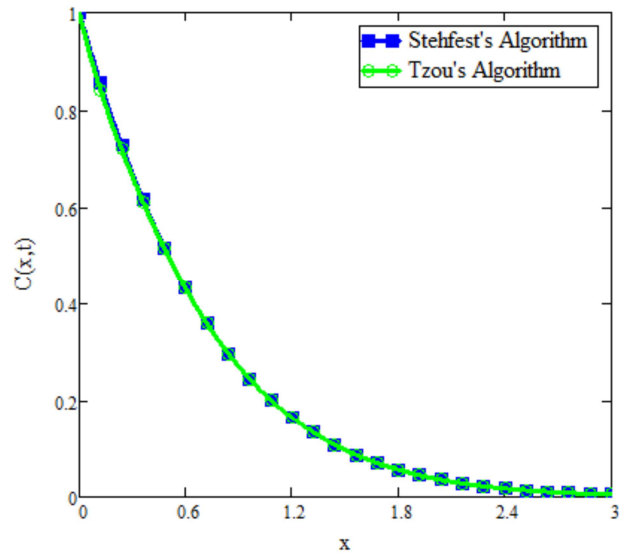


Figure 23. Concentration obtain by Stehfest's and Tzou's Algorithm.

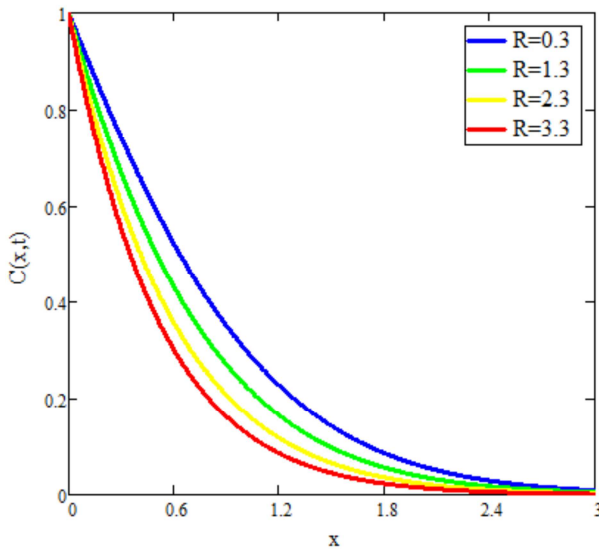


Figure 21. Concentration profile  $C(x,t)$  for parameter  $R$ .

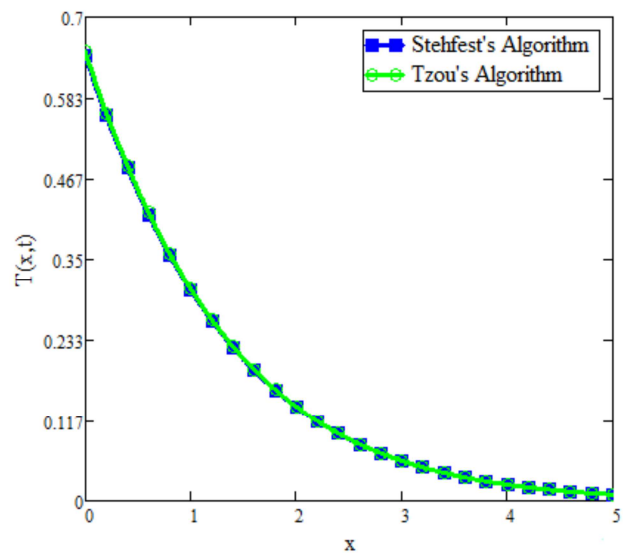


Figure 24. Temperature obtain by Stehfest's and Tzou's Algorithm.

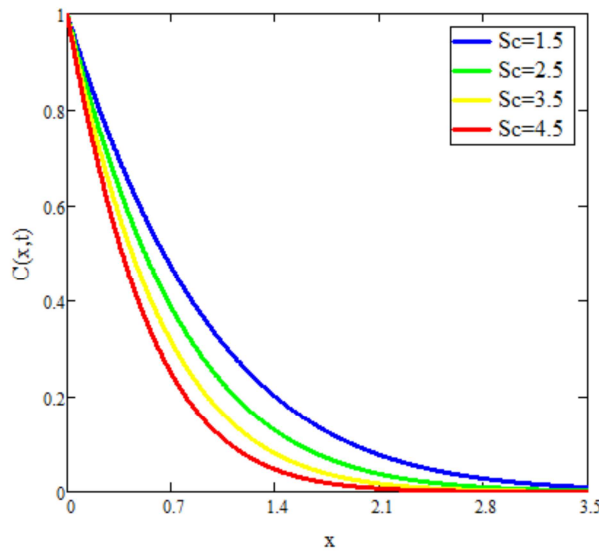


Figure 22. Concentration profile  $C(x,t)$  for parameter  $Sc$ .

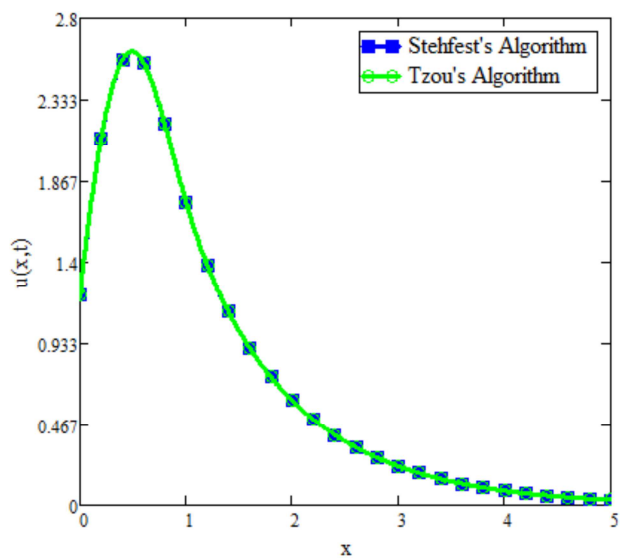


Figure 25. Velocity obtain by Stehfest's and Tzou's Algorithm.

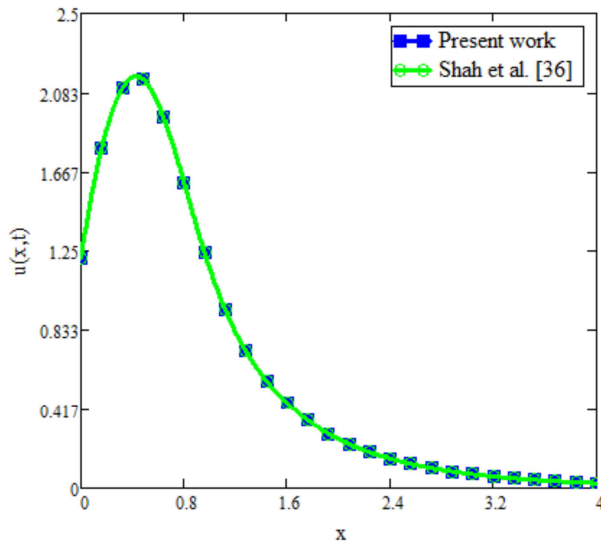


Figure 26. Velocity profile for comparison of our work with Shah et al. [36].

## 6. Conclusion

A magnetohydrodynamics flow of second grade fluid model has been taken and solved using Laplace transform with solution. The conditions of flow problem are satisfied by the results. Different graphs have been plotted for flow parameters and then discussed. The key points of this flow model are:

1. With increasing values of fractional parameter, the velocity distribution slows down.
2. Thermal buoyancy forces accelerate the fluid motion.
3. The velocity of fluid decreases as Schmidt number, magnetic parameter, and heat consumption parameter rises.
4. The fluid velocity is increased for raising values of  $Du$ .
5. The temperature profile increases by the smaller values of  $Pr$ .
6. The temperature profile is a decreasing function of  $\alpha$ .
7. The  $T(x,t)$  is an increasing function of  $Du$ .
8. The concentration profile decreases with larger values of  $Sc$ .
9. The concentration profile reduces with larger values of  $R$ .
10. The concentration level is a decreasing function of  $\alpha$ .

## References

- [1] Kai-Long Hsiao, Combined electrical MHD heat transfer thermal extrusion system using Maxwell fluid with radiative and viscous dissipation effects, *Applied Thermal Engineering*, 112, (2017), 1281-1288.
- [2] N. A. Shah, D. Vieru, C. Fetecau, Effects of the fractional order and magnetic field on the blood flow in cylindrical domains, *Journal of Magnetism and Magnetic Materials*, 409, (2016), 10-19.
- [3] K. Das, Influence of slip and heat transfer on MHD peristaltic flow of a Jeffrey fluid in an inclined asymmetric porous channel, *Indian Journal of Mathematics*, 54, (2012), 19-45.
- [4] M. Qasim, Heat and mass transfer in a Jeffrey fluid over a stretching sheet with heat source/sink, *Alexandria Engineering Journal*, 52, (2013), 571-575.
- [5] M. Ahmad, M. Imran, M. Aleem, I. Khan, A comparative study and analysis of natural convection flow of MHD non-Newtonian fluid in the presence of heat source and first-order chemical reaction, *Journal of Thermal Analysis and Calorimetry*, 137, (2019), 1783-1796.
- [6] A. Atangana, A. Akgul, K. M. Owolabi, Analysis of fractal fractional differential equations, *Alexandria Engineering Journal*, 59, (2020), 1-18.
- [7] D. Baleanu, A. Fernandez, A. Akgul, On a fractional operator combining proportional and classical differintegrals, *Mathematics*, 8, (2020), 360-373.
- [8] S. G. Kumar, R. K. Kumar, G. V. Kumar, S. V. K. Varma, Soret and radiation effects on MHD free convection slip flow over an inclined porous plate with heat and mass flux, *Advanced Science, Engineering and Medicine*, 8, (2016), 1-10.
- [9] N. Sandeep, M. S. J. Kumar, Heat and mass transfer in nano fluid flow over an inclined stretching sheet with volume fraction of dust and nanoparticles, *Journal of Applied Fluid Mechanics*, 9, (2016), 2205-2215.
- [10] M. U. Ahammad, M. H. Rashid, M. Obayedullah, Radiation effect with Eckert number and Forchheimer number on heat and mass transfer over an inclined plate in the influence of suction/injection flow, *Asian Research Journal of Mathematics*, 7, (2017), 1-11.
- [11] F. Ali, I. Khan, Samiulhaq, S. Shaffe, Conjugate effects of heat and mass transfer on MHD free convection flow over an inclined plate embedded in a porous medium, *Plos One*, 8, (2013), 110-124.
- [12] M. F. Sayeda, N. S. Elgazeryb, Effect of variations in viscosity and thermal diffusivity on MHD heat and mass transfer flow over a porous inclined radiate plane, *The European Physical Journal Plus*, 124, (2011), 126-142.
- [13] G. Bogнар, I. Gombkoto, K. Hricz, Non-Newtonian fluid flow down an inclined plane, *Recent Advances in Fluid Mechanics and Heat and Mass Transfer*, 26, (2011), 225-240.
- [14] M. Khan, H. Sardar, M. M. Gulzar, A. S. Alshomrani, On multiple solutions of non-Newtonian Carreau fluid flow over an inclined shrinking sheet, *Results in Physics*, 8, (2018), 926-932.
- [15] N. A. Sheikh, D. L. C. Ching, I. Khan, D. Kumar, K. S. Nisar, A new model of fractional Casson fluid based on generalized Fick's and Fourier's laws together with heat and mass transfer, *Alexandria Engineering Journal*, 59 (2020), 2865-2876.
- [16] M. A. M. Ahmed, M. E. Mohammed, A. A. Khidir, On linearization method to MHD boundary layer convective heat transfer with flow pressure gradient, *Propulsion and Power Research*, 4, (2015), 105-113.
- [17] P. V. S. Narayana, Effects of variable permeability and radiation absorption on magnetohydrodynamic (MHD) mixed convective flow in a vertical wavy channel with traveling thermal waves, *Propulsion and Power Research*, 4, (2015), 150-160.
- [18] M. Ramzan, A. Shafique, M. Amir, M. Nazar, Z. U. Nisa, MHD flow of fractionalized Jeffrey fluid with Newtonian heating and thermal radiation over a vertical plate, *International Journal of Sciences: Basic and Applied Research*, 61, (2022), 170-195.

- [19] A. Khan, K. A. Abro, A. Tassaddiq, I. Khan, Atangana Baleanu and Caputo Fabrizio analysis fractional derivatives for heat and mass transfer of second grade fluids over a vertical plate, *Entropy*, 19, (2017), 279-281.
- [20] A. Khan, I. Khan, F. Ali, S. Shafie, Effects of wall shear stress MHD conjugate flow over an inclined plate in a porous medium with ramped wall temperature, *Mathematical Problems in Engineering*, (2014), 1-15.
- [21] G. S. Seth, A. K. Singha, R. Sharma, MHD natural convection flow with hall effects, radiation and heat absorption over an exponentially accelerated vertical plate with ramped temperature, *Indian Journal of Scientific Research and Technology*, 3, (2015), 10-22.
- [22] M. D Tran, V. Ho, H. N. Van, On the stability of fractional differential equations involving generalized Caputo fractional derivative, *Mathematical Problems in Engineering*, (2020), 1-14.
- [23] N. H. Tuan, H. Mohammadi, S. Rezapour, A mathematical model for COVID-19 transmission by using the Caputo fractional derivative, *Chaos Solitons Fractals*, 140, (2020), 1-12.
- [24] Y. Liu, B. Guo, Effects of second order slip on the flow of fractional Maxwell MHD fluid, *Journal of the association of arab universities for basic and applied sciences*, 24 (2017), 232-241.
- [25] M. Ramzan, Z. U. Nisa, M. Ahmad, M. Nazar, Flow of Brinkman fluid with heat generation and chemical reaction, *Complexity*, (2021), 1-11.
- [26] Z. A. Khan, S. U. Haq, T. S. Khan, I. Khan, I. Tlili, Unsteady MHD flow of a Brinkman type fluid between two side walls perpendicular to an infinite plate, *Results in Physics*, 9 (2018), 1602-1608.
- [27] F. Ali, S. Shafie, N. Musthapa, Heat and mass transfer with free convection MHD flow past a vertical plate embedded in a porous medium, *Mathematical Problems in Engineering*, 3, (2013), 1-14.
- [28] I. Ahmad, M. Nazar, M. Ahmad, Z. Nisa, N. A. Shah, MHD-free convection flow of CNTs differential type nanofluid over an infinite vertical plate with first-order, chemical reaction, porous medium, and suction/injection, *Mathematical Methods in the Applied Sciences*, (2020), 1-13.
- [29] N. A. Sheikh, D. L. C. Ching, M. Aleem, D. Kumar, K. S. Nisar, A new model of fractional Casson fluid based on generalized Fick's laws and Fourier's laws together with heat and mass transfer, *Alexandria Engineering Journal*, 59 (2020), 2865-2876.
- [30] T. N. Ahmad, I. Khan, Entropy generation in C6H9NAO7 fluid over an accelerated heated plate, *Frontiers in Physics*, 8 (2020), 1-9.
- [31] F. Ali, M. Gohar, I. Khan, MHD flow of water based Brinkman type nanofluid over a vertical plate embedded in a porous medium with variable surface velocity, temperature, and concentration, *Journal of Molecular Liquids*, 223 (2016), 412-419.
- [32] A. Razaq, N. Raza, Heat and mass transfer analysis of Brinkman type fractional nanofluid over a vertical porous plate with velocity slip and Newtonian heating, *Journal of Mathematics*, 51 (2019), 45-69.
- [33] G. S. Blair, J. Caffyn, Significance of power law relation in rheology, *Nature*, 155 (1955), 171-172.
- [34] Y. Povstenko, *Fractional thermoelasticity, solid mechanics and its applications*, Springer International Publishing, (2015), 1-219.
- [35] J. Hristov, *Derivatives with non-singular kernels, From the Caputo-Fabrizio definition and beyond, appraising analysis with emphasis on diffusion model*, *Frontiers in fractional calculus*, first edition Sharjah, United Arab Emirates, Bentham Science Publishers, (2017), 269-340.
- [36] N. A. Shah, A. A. Zafar, S. Akhtar, General solution for MHD free convection flow over a vertical plate with ramped wall temperature and chemical reaction, *Arabian Journal of Mathematics*, 7 (2018), 49-60.
- [37] D. Y. Tzou, *Macro to microscale heat transfer: the lagging behavior*. Washington, District of Columbia: Taylor and Francis, (1997), 01-339.
- [38] H. Stehfest, Algorithm 368: Numerical inversion of Laplace transform. *Communication of Advanced Composit Material*, 13 (1970), 47-49.